AD-A119 365 BATTELLE COLUMBUS LABS OH F/G 17/2
NRL SYNTHETIC HETERODYNE PROCESSOR.(U)
SEP 82 N00014-82-C-2159
UNCLASSIFIED NL

END
DATE FILMED
10-82
DTIC

AD A119365

(12)

Battelle
Columbus Laboratories
505 King Avenue
Columbus, Ohio 43201
Telephone (614) 424-6424
Telex 24-5454

September 2, 1982

DTIC
ELECTE
SEP 16 1982
S D
B

Richard G. Priest
Attn: Code 6510.2
Naval Research Laboratory
4555 Overlook Avenue S.W.
Washington, D. C. 20375

Dear Richard:

Contract Number: N00014-82-C-2159

This is the first bimonthly technical report on the NRL Synthetic Heterodyne Signal Processor. At the time of writing we are about to test a breadboarded version of NRL's Differentiate and Cross-Multiply circuit with a special low-noise signal generator which synthesizes the action of the synthetic heterodyne signal processor.

The time spent on this project so far has been mainly devoted to assembling a stock of electronic components, designing and constructing low-noise amplifiers for use with our spectrum analyzer, designing and constructing the low-noise signal generator, which will be described shortly, and investigating the availability of certain key components required in a compact signal processor. What follows is a brief description of this work.

Figure 1 shows a low-noise pre-amplifier we have built to improve our ability of being able to resolve very small phase deviations. Since the noise figure of our HP 8553B (1 KHz-110 MHz) spectrum analyzer R.F. plug-in is 24 dB, we had hoped to lower the overall noise figure to about 4 dB. Plessey, the manufacturer of the SL 550C video amplifier, specify a noise figure of 3.5 dB. Our measurements indicate a noise figure of

DTIC FILE COPY

DISTRIBUTION STATEMENT A
Approved for public release;
Distribution Unlimited

82 09 07 039

7.5 dB. We cannot account for the discrepancy save for the fact that the devices used may be somewhat noisier than the data sheet would have us believe.

We have had better luck with the Anzac AM-113 amplifier shown in Figure 2. The specifications quoted in the caption are measured parameters and correspond to Anzac's published data.

Figure 3 shows a low-noise low-frequency amplifier used for lowering the noise figure of our HP 8556A LF plug-in. This circuit has not yet been optimized.

In Table 1 we have listed some of the most significant spectral components produced by the synthetic heterodyne modulation process. We are particularly interested in the components at frequencies Wp $\pm$ Wm and 2 Wp $\pm$ Wm. The schematic of Figure 4 shows the basic construction of the signal generator we have built (but not yet fully tested) to synthesize the above signals.

The circuit is basically a frequency modulator followed by a delay-line frequency discriminator. The input to the summing board consists of four signals:

A Manual Phase Adjust which varies the static phase difference between the inputs to the Phase Detector (PD).

A Fading Signal at very low frequencies and large deviations which simulates the large temperature-driven phase fluctuations.

An Acoustic Signal at small deviations which simulates the acoustic signal being received.

A Synthetic Heterodyne Pilot Signal which simulates the pilot-tone placed on the optical carrier by the PZT transducer ($\Delta\Theta p \approx 2.6$ radians).

The summed signals drive an Epicap (variable capacitance) diode which is part of the tuned circuit of a Vackar dual-gate mosfet 30 MHz oscillator. This voltage controlled oscillator (VCO) is fed straight to a Power Divide, which, via driver stages, feeds the Phase Detector (PD) directly and via a coaxial delay line ($\tau \approx 1$ μS). Alternatively,

the VCO (oscillating at a higher frequency) may drive a Double Balanced Mixer (DBM) to increase the percentage frequency deviation. A typical crystal frequency (XTAL) might be 100 MHz. The Low-Pass Filter (LPF) is required to reject the sum frequency component. The output of the Phase Detector (PD) is Low-Pass Filtered (LPF) and the output represents the signal we would obtain from the photodetector in a synthetic heterodyne interferometer.

Figure 5 illustrates our dynamic range considerations. The signal generator is capable of driving the Phase Detector at +15 dBm, though the device is optimized for a +7 dBm drive level. We have measured the wide-band noise floor of the VCO drive to the Phse Detector to be at a level of ~-160 dBm/Hz. Thus, the potential dynamic range at +7 dBm drive is approximately 167 dB, allowing us to detect phase deviations of 10^{-8} radians/$\sqrt{Hz}$.

Figures 6 and 7 show the circuitry of this signal generator, though some component values have yet to be optimized. Low-noise metal film resistors are used in critical stages to reduce the amount of 1/f flicker noise. We have not yet measured the phase noise close to the carrier, but we expect it to be fairly low.

Finally, Figures 8 and 9 show the NRL synthetic heterodyne differentiate α cross-multiply circuit which we have breadboarded and will test shortly, using the above low-noise signal generator.

I leave for the U.K. today for a vacation, but will be back at Battelle on September 22. I shall be pleased to discuss any aspects of the work reported here and our plans for the future after that date.

Yours sincerely,

Stuart Kingsley
Principal Research Scientist

SK/sp

cc: Administrative Contracting Officer (1)
Director, NRL Code 2627 Washington DC 20375 (6)
Defense Technical Information Center (12)

DTIC COPY INSPECTED 2

Accession For
NTIS GRA&I ☑
DTIC TAB ☐
Unannounced ☐
Justification PER LETTER
By
Distribution/
Availability Codes
Dist | Avail and/or Special
A

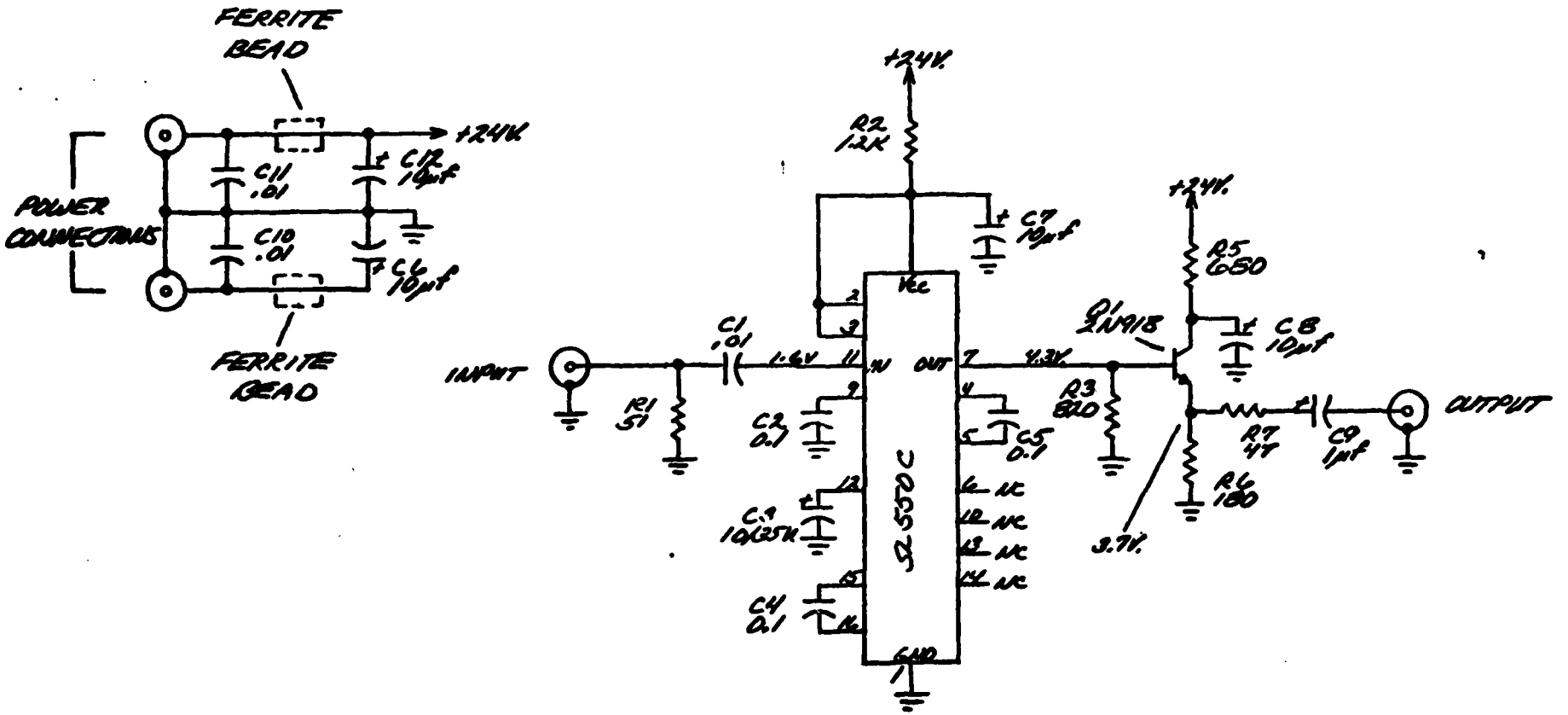

Figure 1. Low-noise pre-amplifier with a 7.5 dB noise figure, 36 dB gain, 0 dBm 1 dB compression point and a 100 KHz to 180 MHz 3dB bandwidth

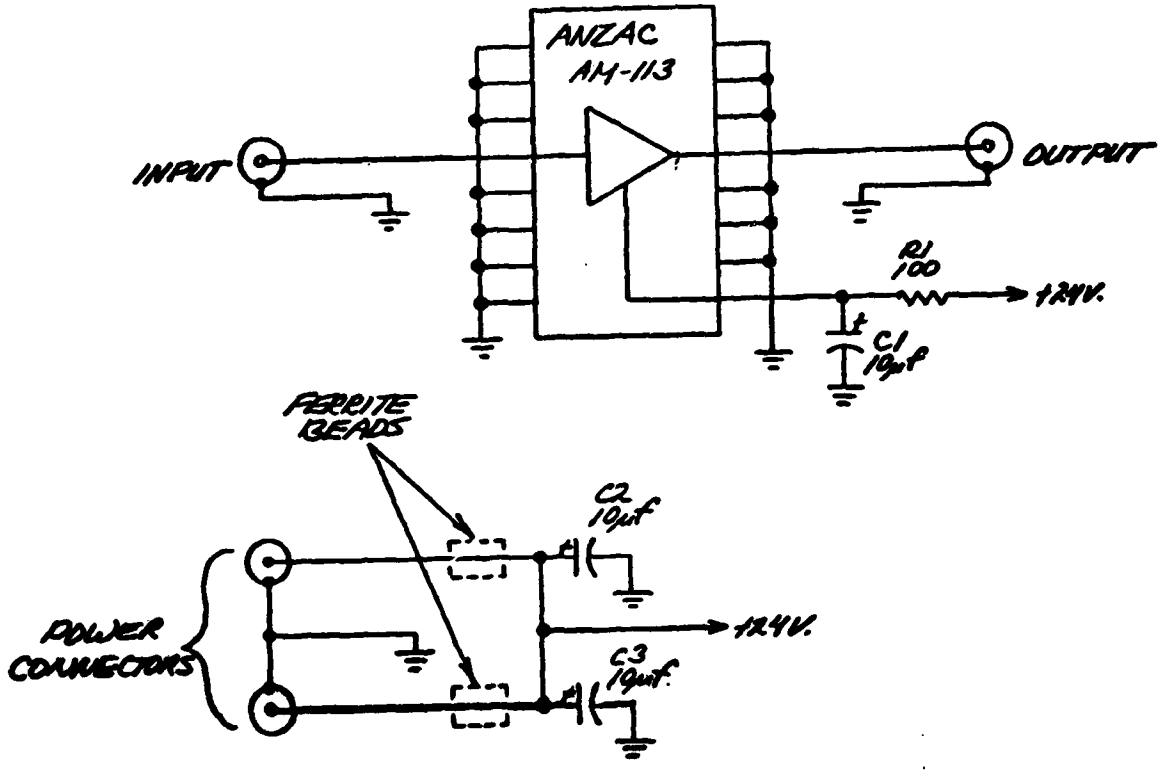

Figure 2. Low-noise pre-amplifier with a 1.5 dB noise figure, 30 dB gain, +19 dBm 1 dB compression point and a 5 MHz to 210 MHz 3 dB bandwidth

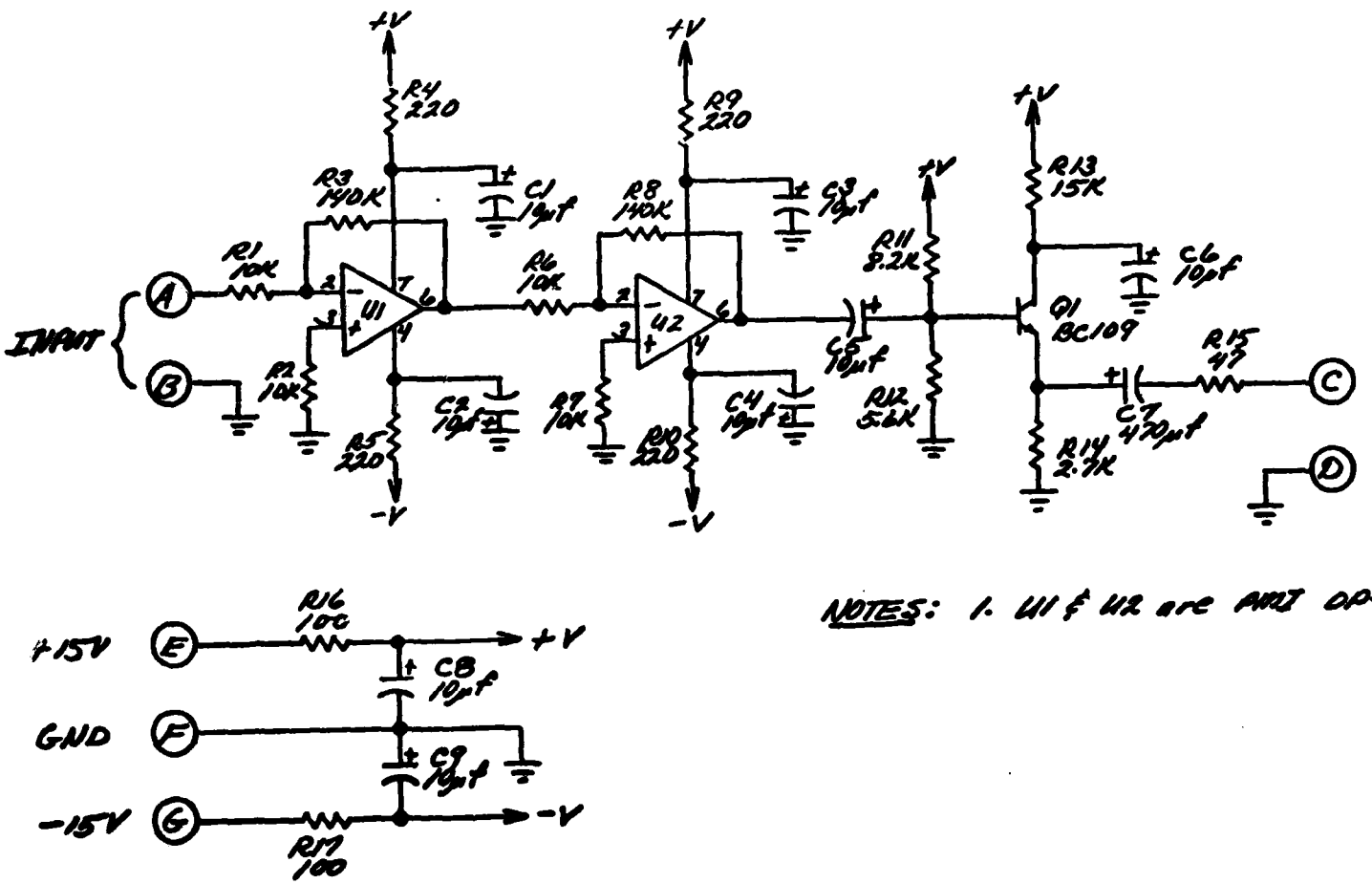

Figure 3. Low-noise low-frequency pre-amplifier

Table 1. Some significant spectral components produced by phase-detecting a two-tone phase-modulated carrier

Frequency	Spectral component
0	$\frac{1}{2}[1 + J_0(\Delta\phi_p)J_0(\Delta\phi_m)\cos\phi]$
ω_m	$J_0(\Delta\phi_p)J_1(\Delta\phi_m)\ \sin\phi\cdot\sin\omega_m t$
$2\omega_m$	$J_0(\Delta\phi_p)J_2(\Delta\phi_m)\cos\phi\cdot\cos 2\omega_m t$
ω_p	$J_1(\Delta\phi_p)J_0(\Delta\phi_m)\sin\phi\cdot\sin\omega_p t$
$\omega_p \pm \omega_m$	$J_1(\Delta\phi_p)J_1(\Delta\phi_m)\cos\phi\cdot[\cos(\omega_p + \omega_m)t - \cos(\omega_p - \omega_m)t]$
$\omega_p \pm 2\omega_m$	$J_1(\Delta\phi_p)J_2(\Delta\phi_m)\sin\phi\cdot[\sin(\omega_p + 2\omega_m)t + \sin(\omega_p - 2\omega_m)t]$
$2\omega_p$	$J_2(\Delta\phi_p)J_0(\Delta\phi_m)\cos\phi\cdot\cos 2\omega_p t$
$2\omega_p \pm \omega_m$	$J_2(\Delta\phi_p)J_1(\Delta\phi_m)\sin\phi\cdot[\sin(2\omega_p + \omega_m)t - \sin(2\omega_p - \omega_m)t]$
$2\omega_p \pm 2\omega_m$	$J_2(\Delta\phi_p)J_2(\Delta\phi_m)\cos\phi\cdot[\cos(2\omega_p + 2\omega_m)t + \cos(2\omega_p - 2\omega_m)t]$

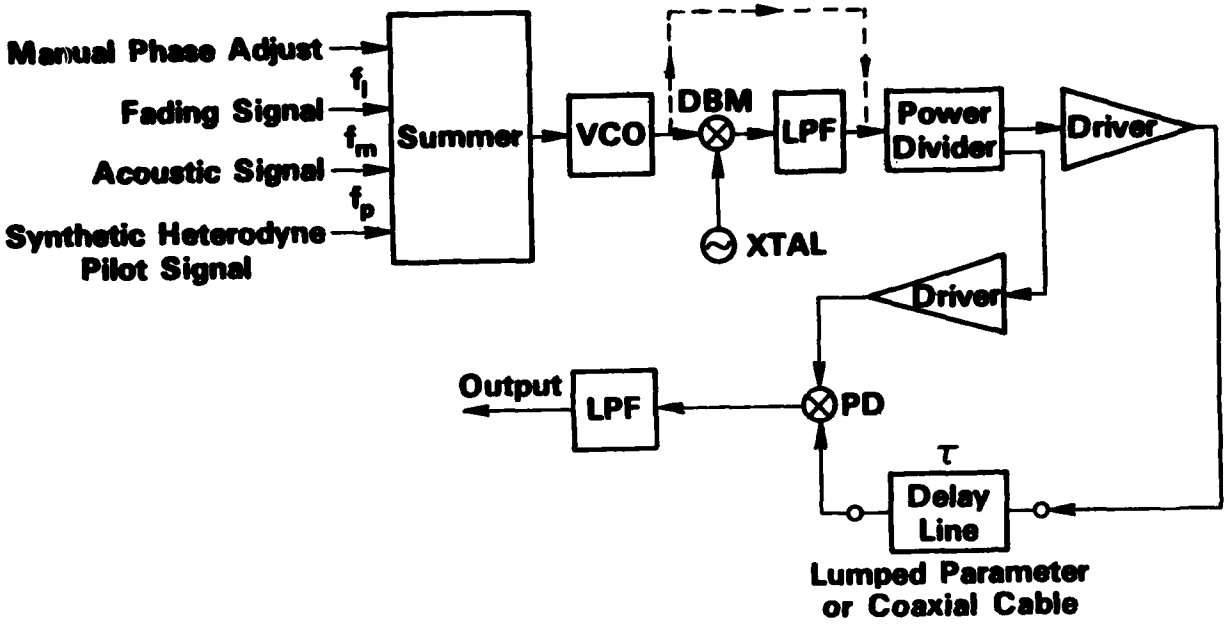

Figure 4. Basic construction of the signal generator which synthesizes the action of a synthetic heterodyne interferometer.

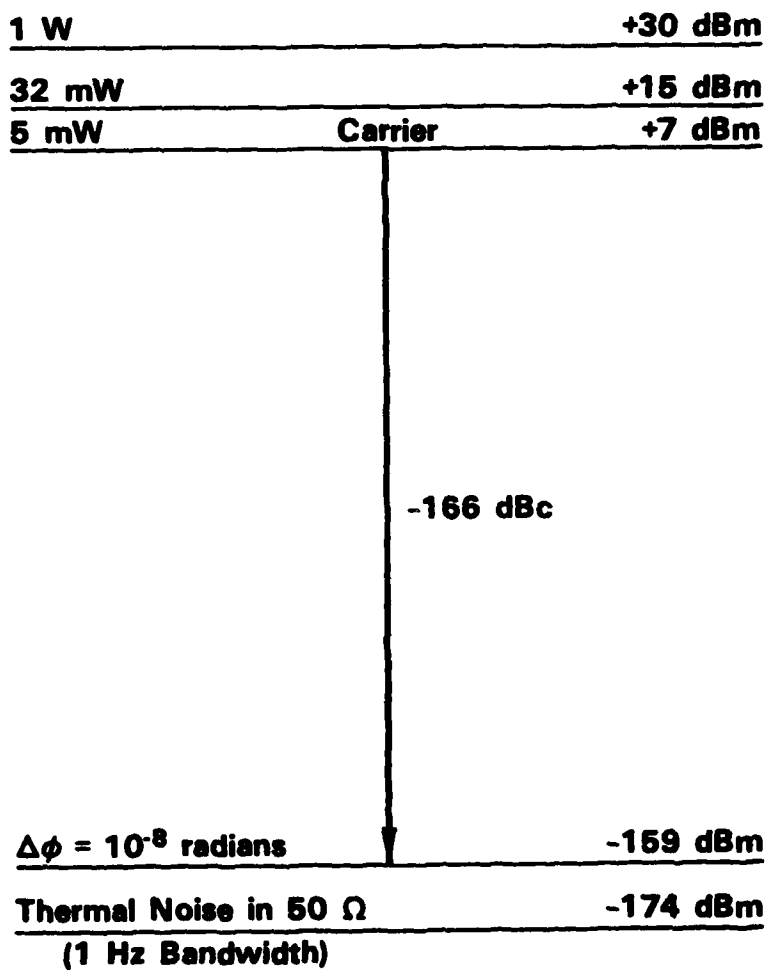

Figure 5. Dynamic range considerations in phase modulation systems.

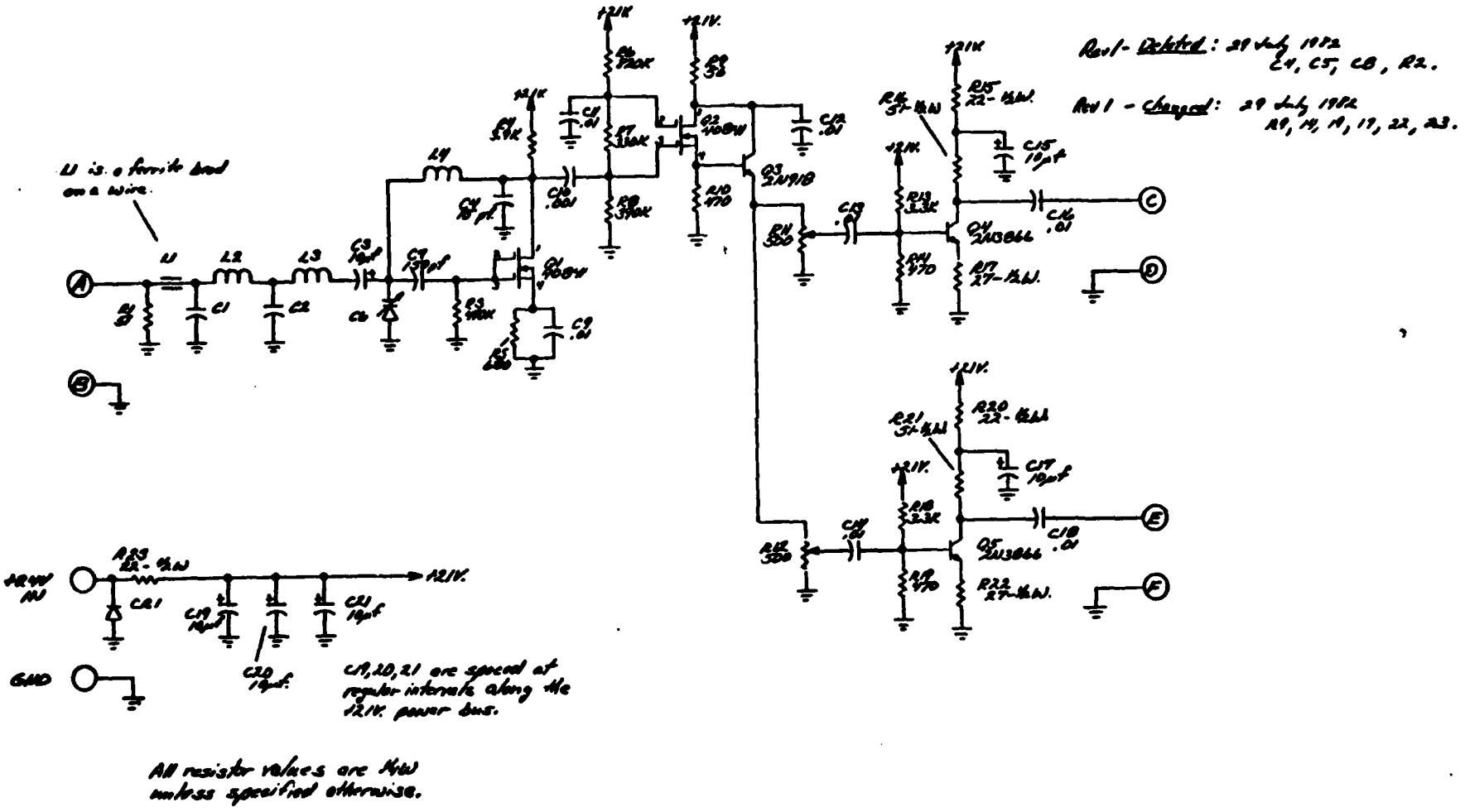

Figure 6. Very low-noise signal generator for synthesizing signals produced by a synthetic heterodyne interferometer. This diagram shows the VCO and driver stages

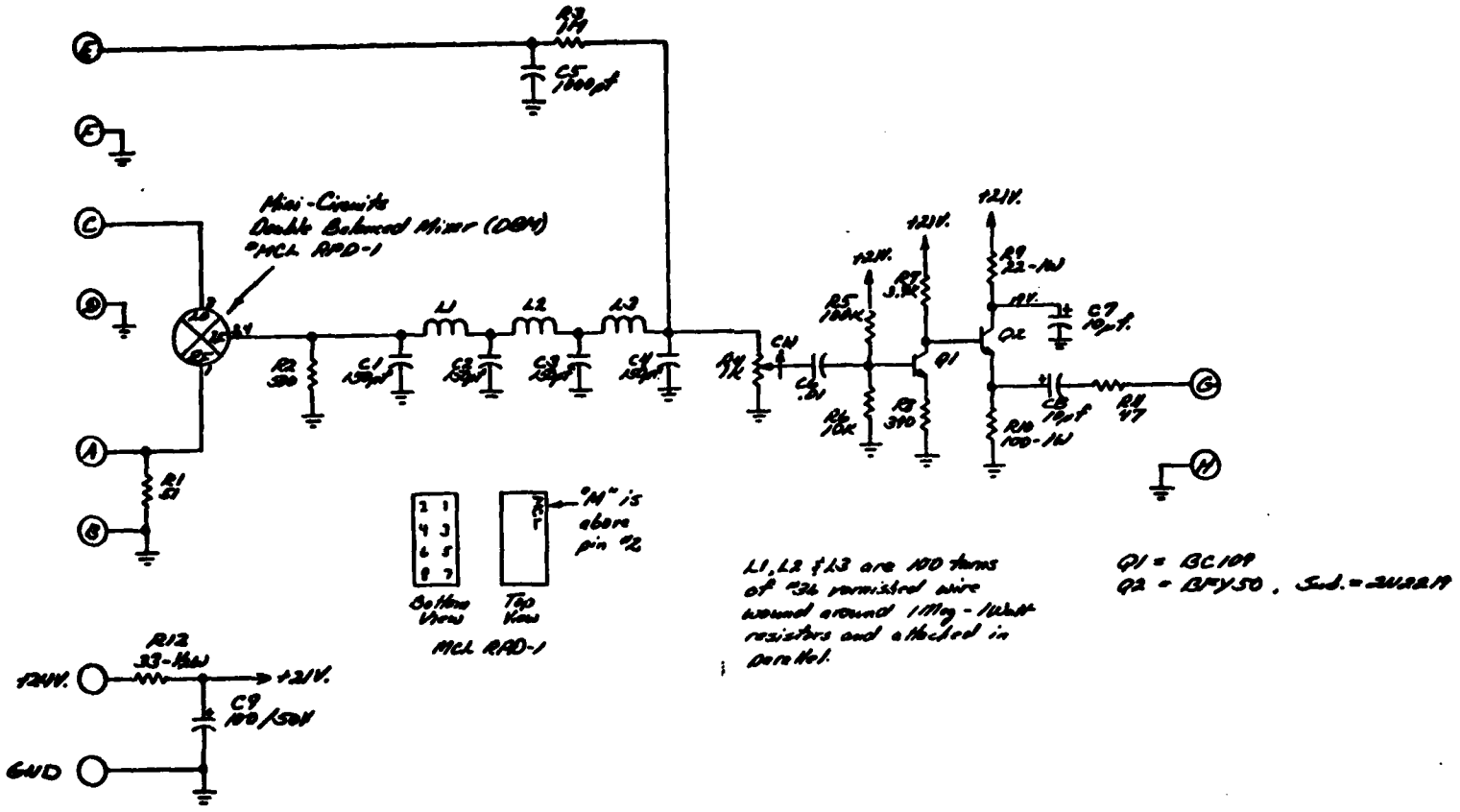

Figure 7. Very low-noise signal generator for s
signals produced by a synthetic heter
ferometer. This diagram shows the phas detector,
low-pass filter and output stage

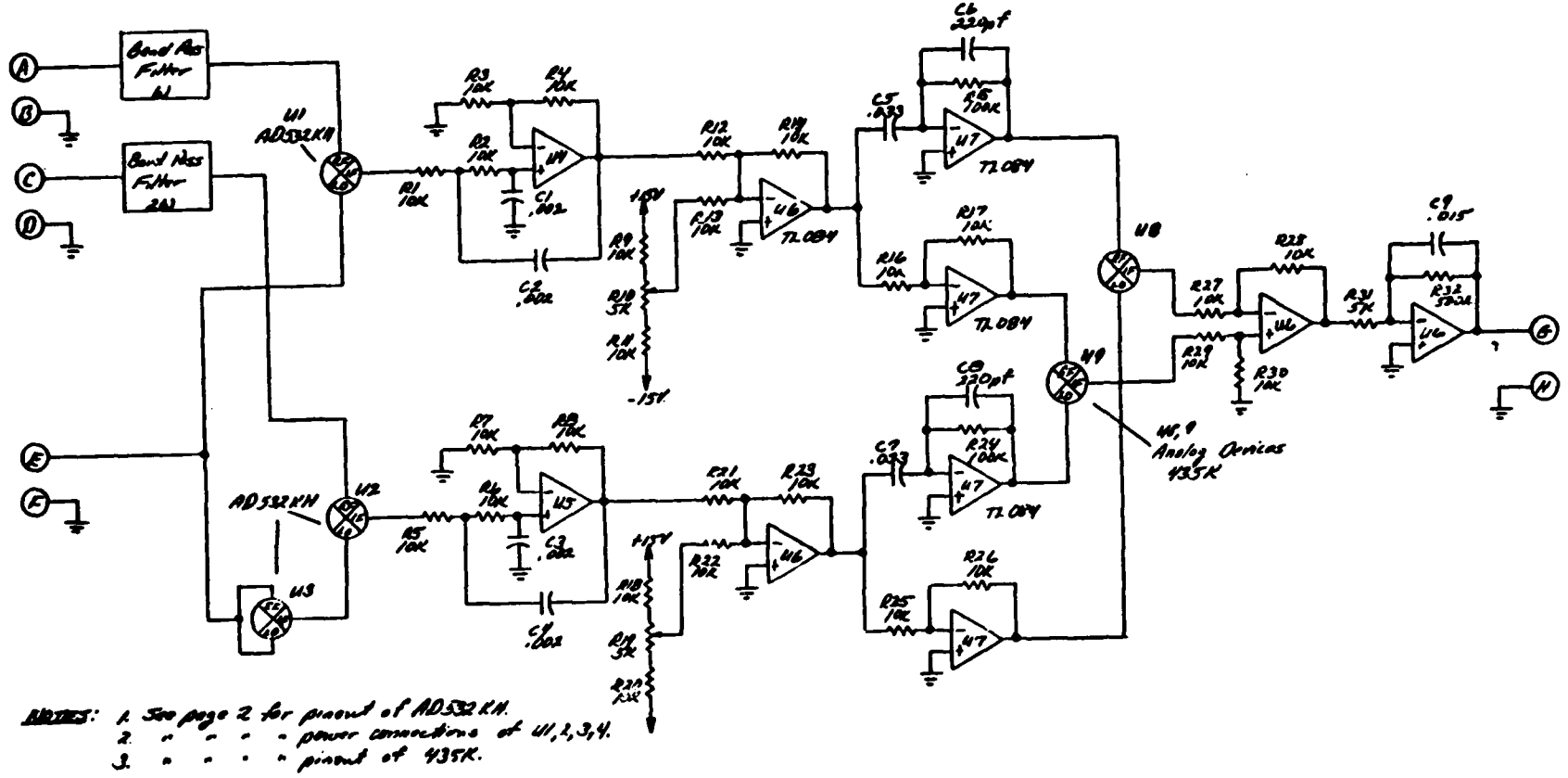

Figure 8. The NRL differentiate and cross-multiply signal processor

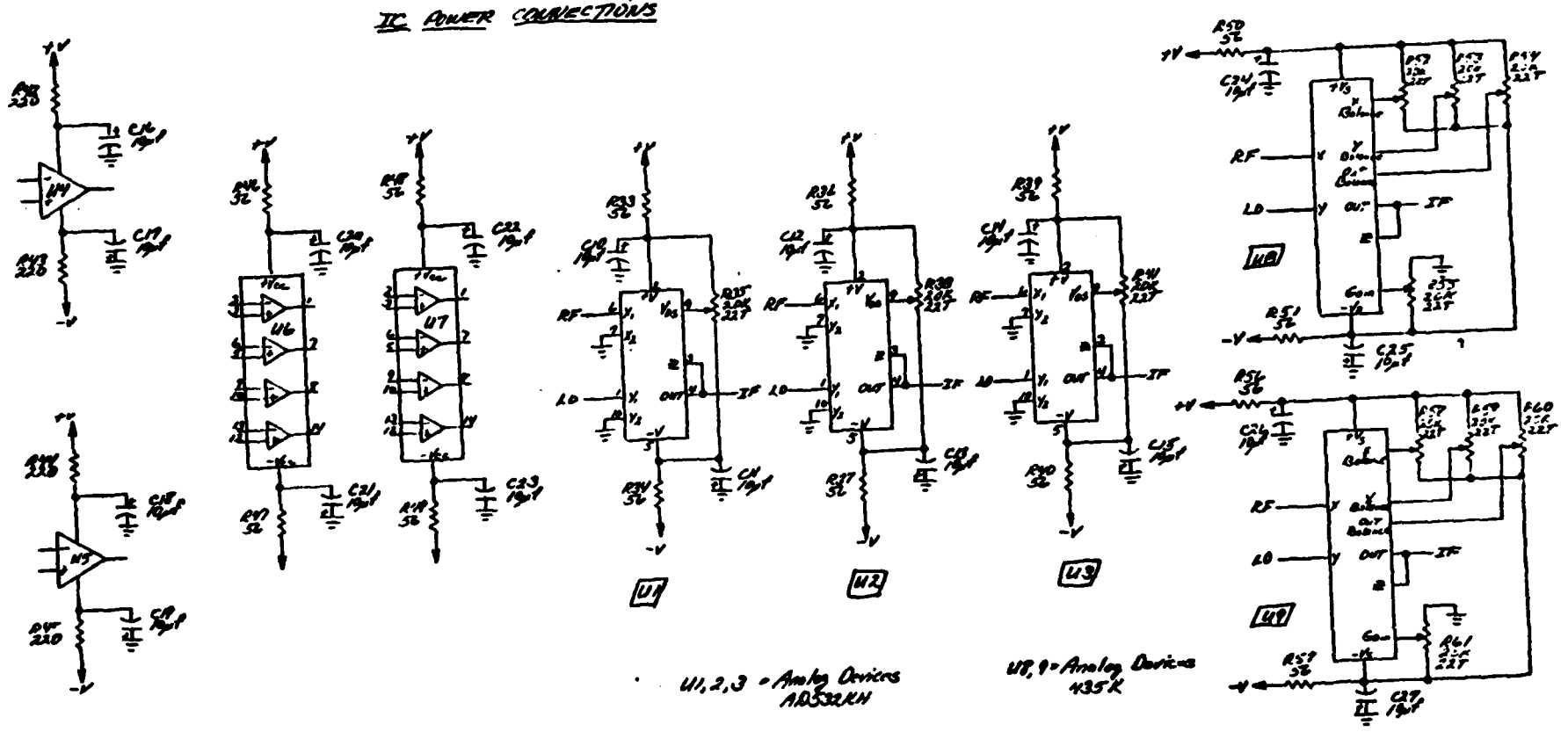

Figure 9. The NRL differentiate and cross-multiply signal processor


DATE
ILME
8